INDIAN JOURNAL OF SCIENCE AND TECHNOLOGY

ORIGINAL ARTICLE

Seismic Response of Multi-Storey RCC Buildings with Lead Rubber Bearing Isolators under Aging Effects

Adersha Babu[1], **R K Chethan Gowda**[1]*

1 Department of Civil Engineering, M S Ramaiah University of Applied Sciences, Bengaluru, Karnataka – 560054, India

OPEN ACCESS

Received: 09/09/2026

Accepted: 30/09/2026

Published: 16/11/2026

Citation: Babu A, Chethan Gowda RK (2026) Seismic Response of Multi-Storey RCC Buildings with Lead Rubber Bearing Isolators under Aging Effects. Indian Journal of Science and Technology 19(41): 2804-2816. https://doi.org/10.17485/IJST/v19i41.1262

* **Corresponding author**.

chethangowdark.ce.et@msruas.ac.in

Funding: None

Competing Interests: None

Copyright: © 2026 Babu & Chethan Gowda. This is an open access article distributed under the terms of the Creative Commons Attribution License, which permits unrestricted use, distribution, and reproduction in any medium, provided the original author and source are credited.

Published By Indian Society for Education and Environment (iSee)

ISSN
Print: 0974-6846
Electronic: 0974-5645

Abstract

Objectives: To quantify how aging of Lead Rubber Bearings (LRBs) alters the seismic response of multi-storey reinforced cement concrete (RCC) buildings of different heights and to derive height-specific aging modification factors. **Method**: G+10 and G+15 RCC frames were analyzed in ETABS 2018 by equivalent-linear Response Spectrum Analysis as per IS 1893 (Part 1): 2016, Zone V, with two isolators: LRB 1 (bilinear, proportioned for each height) and LRB 2 (multilinear, common to both). Aging of 0–30% (5% steps) was modeled by modifying both isolator properties at every level, increasing the effective stiffness (λ_K = 1.00–1.30) and reducing the effective damping (λ_ξ = 1.00–0.70) by equal percentages; aging factors are aged-to-healthy response ratios. **Findings**: Healthy LRB 1 reduced base shear by 54.0% (G+10) and 44.2% (G+15) relative to the fixed-base models. At 30% aging, the LRB 1 factors were 1.107 (G+10) and 1.100 (G+15) for base shear, 1.107 and 1.088 for inter-storey drift, about 1.10 for column forces and 0.910 and 0.935 for roof displacement, leaving residual base shear reductions of 49.1% and 38.6%. Beams at the isolation level were the most aging-sensitive members: beam moment factors reached 1.116 (G+10) and 1.113 (G+15), the highest of any response, and in the G+15 building beam shear exceeded the fixed-base value from 5% aging onwards. These factors reflect the combined effect of the stiffness increase and the damping reduction and are approximate equivalent-linear indicators valid only within the range studied. **Novelty**: Bearing-level aging is converted into height- and configuration-specific building response factors, showing that design based on as-manufactured properties underestimates late-life forces by about 10%, with isolation-level beams most affected.

Keywords: Lead Rubber Bearing; Base Isolation; Aging Effects; Seismic Response; Property Modification Factors

1 Introduction

Base isolation places flexible bearings between the foundation and the superstructure, lengthening the fundamental period and reducing the seismic forces transmitted to the frame. In the widely used Lead Rubber Bearing (LRB), laminated rubber supplies lateral flexibility and a lead core dissipates energy by hysteresis. Building-level studies confirm this effectiveness but show that it depends on the bearing properties and on the superstructure. Ziraoui et al.[(1)] found that LRBs reduced the seismic response of eight- and ten-storey reinforced cement concrete (RCC) buildings by 50–70%. By varying the initial stiffness and yield strength of LRBs beneath a five-storey building, Domadzra et al.[(2)] obtained maximum reductions of 46% in base shear and 65% in inter-storey drift and showed that the response is sensitive to the isolator properties. Kayı et al.[(3)] showed that member dimensions, concrete strength and first-storey height alter the demands on an LRB-retrofitted RCC building; Yanik and Okuroğlu[(4)] compared LRB and high-damping rubber systems in RCC buildings, and Madhukumar et al.[(5)] evaluated LRB isolation in low-, medium- and high-rise RCC buildings. These studies address the as-designed isolation system, not the long-term aging of the bearings.

Bearing properties, however, change with time. Guzmán Sánchez et al.[(6)] reported that the natural rubber compounds used in bearings change their mechanical response after thermal aging, Li et al.[(7)] quantified LRB degradation under alternating aging and seawater attack, and Velasco-Cuervo et al.[(8)] reported the property changes of low-cost isolator prototypes after aging and at low temperature. These material- and device-level studies stop at the bearing. At the building level, Calabrese et al.[(9)] assessed aging of fiber-reinforced bearings beneath a single low-rise residential building, so their findings cannot be applied directly to LRBs or taller frames, and Xue et al.[(10)] developed an LRB hysteresis model with coupled thermal and mechanical responses, showing that bearing properties do not remain at their nominal values.

Three gaps therefore remain: (i) device-level aging is rarely propagated to storey drift, base shear and member forces; (ii) building-level evidence for conventional buildings is limited to one height and one bearing type; and (iii) no study describes how the aging penalty scales with building height. Height matters because a taller frame has a longer fixed-base period, so the period shift achieved by isolation, and hence the margin available before aging consumes it, is smaller. This study addresses these gaps through a parametric analysis of G+10 and G+15 RCC buildings with two LRB configurations at seven aging levels (0–30%). It provides height- and configuration-specific aging modification factors (ratio of aged to healthy response) that link the bearing property modification factors (λ_K, λ_ξ) to the building response and can be used in long-term design checks within the range studied.

2 Methodology

2.1 Building configuration and design data

Two symmetric RCC moment-resisting frames, G+10 (33 m) and G+15 (48 m), were considered with the same plan (25 m × 25 m, five bays of 5 m in each direction) and storey height (3.0 m), so that the comparison reflects height and isolator properties rather than plan geometry. M30 concrete and Fe500 steel were used. The G+10 building has 300 mm × 650 mm beams and columns reducing from 650 mm × 650 mm (ground to third floor) to 450 mm × 450 mm (eighth to tenth floor); the G+15 building has 300 mm × 700 mm beams and columns reducing from 700 mm × 700 mm (ground to third floor) to 500 mm × 500 mm (tenth to fifteenth floor). Both have 150 mm slabs, 230 mm external and 115 mm internal walls, a floor finish of 1.5 kN/m^2 and a live load of 3 kN/m^2. The IS 1893 (Part 1): 2016 parameters for Zone V were adopted: Z = 0.36, I = 1.2, R = 5 and medium soil (Type II).

2.2 Analysis procedure and baseline model

Each model was built in ETABS 2018 as a three-dimensional frame with a rigid diaphragm at each floor. After modal analysis, Response Spectrum Analysis (RSA) was performed with the 5%-damped design spectrum of IS 1893 (Part 1): 2016 for Zone V and medium soil, and the modal responses were combined by the Complete Quadratic Combination (CQC) method specified in the code. CQC was preferred to the Square Root of Sum of Squares (SRSS) rule because it accounts for the correlation of closely spaced modes: in the healthy G+10 model with LRB 1, the two translational isolation modes (3.29 s) and the torsional isolation mode (3.06 s) lie within 10% of each other, while all higher modes have periods of 0.66 s or less. The same spectrum function and scale factor were used for all models, so the aged-to-healthy ratios are unaffected by spectrum scaling. The fixed-base model of each building is the reference case. The responses compared are roof displacement, maximum inter-storey drift, base shear, the bending moment and shear force in two columns (C1, C2) and in a ground-floor beam at the isolation level (B1; maximum positive moment and maximum shear of the design envelope), and the axial force–biaxial moment (P-M-M)

interaction ratio of C1 and C2. Two criteria are used: the percentage reduction relative to the fixed-base model, and the aging modification factor, i.e. the ratio of the response at a given aging level to the healthy (0%) isolated response.

2.3 LRB 1: height-specific bilinear bearing

LRB 1 is a bilinear bearing proportioned separately for each building for a target isolation period of 3.0 s, since the different masses of the two buildings require different bearing stiffnesses. The lead core provides a post-yield stiffness ratio $\alpha = 0.10$, and the bearing diameter and rubber thickness satisfy the target period (Table 1). The bearings are modeled in ETABS as Rubber Isolator link elements with bilinear hysteretic properties, one beneath each column (36 bearings per building).

2.4 LRB 2: standard multilinear bearing

LRB 2 is a multilinear plastic bearing used unchanged for both buildings, so that the influence of height can be observed without changing the bearing. Since IS 1893 (Part 1): 2016 does not provide design provisions for isolation systems, LRB 2 was designed for a G+10 RCC building using the procedure for seismically isolated structures in ASCE/SEI 7-10, Chapter 17, with the seismic demand taken from the IS 1893 Zone V spectrum for medium soil. The bearing was implemented in ETABS as a multilinear plastic link element following the modeling approach adopted by Haveri et al.[11]; all properties are reported in Table 1 so that the model can be reproduced independently. For a target isolation period of 3.0 s and a design displacement $D_D = 348.16$ mm, the design gives a post-yield stiffness $K_d = 1{,}603.71$ kN/m and a characteristic strength $Q_d = 47.56$ kN. The effective stiffness is the secant stiffness of the bilinear design idealization at D_D: $K_{eff} = K_d + Q_d/D_D = 1{,}603.71 + 47.56/0.34816 = 1{,}740.31$ kN/m. This is approximately equal to the stiffness of LRB 1 for the G+15 building but 48% greater than that for the G+10 building, a difference central to the interpretation of the results.

Table 1. Isolator properties and aging modification factors

Parameter	LRB 1 (G+10)	LRB 1 (G+15)	LRB 2 (both buildings)
Hysteretic model	Bilinear	Bilinear	Multilinear plastic
Bearing diameter (mm)	820	1,004	705
Effective stiffness, K_{eff} (kN/m)	1,178.13	1,738.43	1,740.31
Characteristic strength, Q_d (kN)	32.10	47.37	47.56
Post-yield stiffness ratio, α	0.10	0.10	0.099
Target isolation period (s)	3.0	3.0	3.0
Design displacement for K_{eff}, D_D (mm)	347	347	348.16
Bearings per building	36	36	36
Aging level (%)	0, 5, 10, 15, 20, 25, 30		
Stiffness factor, λ_K	1.00, 1.05, 1.10, 1.15, 1.20, 1.25, 1.30		
Damping reduction factor, λ_ξ	1.00, 0.95, 0.90, 0.85, 0.80, 0.75, 0.70		

2.5 Aging simulation

Seven aging levels were simulated parametrically: 0% (healthy, as-manufactured), 5%, 10%, 15%, 20%, 25% and 30%. At each level the effective horizontal stiffness and the effective damping of every bearing were modified simultaneously. The effective stiffness is multiplied by $\lambda_K = 1 + a$, where a is the aging level expressed as a fraction; this reflects hardening of the rubber through continued cross-linking and oxidation, as reported in material- and device-level aging research[6],[7], and follows Rahman et al.[12], who evaluated the effect of LRB rubber aging on a base-isolated reactor building using a bilinear isolator model. Aging is assumed to act on the rubber only; the characteristic strength of the lead core was not modified, on the assumption that lead, which recrystallizes at ambient temperature, retains its yield properties over time. For simplicity, λ_K was applied to the total effective stiffness, $K_{eff} = K_d + Q_d/D_D$, rather than to the rubber (post-yield) stiffness K_d alone. Because the lead-core term Q_d/D_D is only about 8% of K_{eff} for all three bearings (Table 1), a rubber-only scaling would give an effective stiffness factor of $1 + 0.92a$, i.e. 1.28 instead of 1.30 at 30% aging. The adopted scaling therefore slightly overstates the stiffness increase, making the force and drift factors marginally conservative and the displacement reductions marginally overestimated; for this reason, the isolation gap should be sized using the healthy displacement (Section 3.5). Stiffening of the rubber also lowers the equivalent damping of the bearing, since the energy dissipated by the lead core stays nearly constant while K_{eff} rises. The damping was therefore reduced by the same percentage, $\lambda_\xi = 1 - a$ (Table 1): 5% aging corresponds to

+5% stiffness and −5% damping, and 30% aging to $K_{eff,aged}$ = 1.30 $K_{eff,0\%}$ with the damping reduced to 70% of its 0% value. For LRB 1 of the G+10 building, the effective stiffness rose from 1,178.13 to 1,531.57 kN/m and the effective damping of the link fell from 0.050 to 0.035 kN·s/m. The same procedure was applied to LRB 1 and LRB 2 in both buildings; in addition to the two fixed-base models, 28 healthy or aged isolated cases were analyzed by updating both link properties, repeating the modal analysis and rerunning the RSA.

2.6 Equivalent-linear representation and damping

Because RSA is linear, each isolator link enters it only through its effective stiffness K_{eff} and effective damping; the bilinear (LRB 1) and multilinear (LRB 2) force–displacement relations would be used only in a nonlinear analysis and do not affect the results reported here. The healthy bearing displacements from the RSA (51.51–65.02 mm, Table 2) are design-level values obtained with the reduced design spectrum and are therefore not directly comparable with D_D; because K_{eff} was not re-evaluated at the actual displacement demand, the effective bearing stiffness is approximate. The effective stiffness and damping were evaluated once, for the healthy bearing, and scaled by λ_K and λ_ξ without iteration at the smaller displacement of the aged bearing, so the coupled, amplitude-dependent change in the properties of a yielding bearing is not captured. The aging modification factors are therefore approximate parametric indicators derived from equivalent-linear analysis, not exact nonlinear demands.

The same 5%-damped design spectrum of IS 1893 (Part 1): 2016 and the same load-case definition were used for every model; no damping-dependent spectral modification factors or composite (e.g., strain-energy-weighted) modal damping were applied. Aging enters only through the isolator link properties, and each aging modification factor is the ratio of the response of the aged model, with both property changes applied, to that of the healthy model. Every reported factor therefore reflects the combined effect of the stiffness increase and the damping reduction; the separate contributions of the two changes were not quantified (Section 4).

3 Results and Discussion

3.1 Healthy isolation: fixed-base versus isolated response

The healthy response is summarized in Figure 1 and Table 2. Because deformation concentrates at the isolation plane, the superstructure translates almost as a rigid body: 65.02 mm of the 84.33 mm roof displacement of the G+10 building with LRB 1, and 63.53 mm of the 96.38 mm roof displacement of the G+15 building, occur across the bearings. The maximum inter-storey drift above the first storey is correspondingly reduced, by 50.4% and 41.9% (G+10, LRB 1 and LRB 2) and by 36.8% and 27.5% (G+15). The first storey, directly above the isolation plane, behaves differently (Figure 1b, d): its drift in the isolated models is 1.57 and 1.87 $\times$ 10^{-3} (G+10, LRB 1 and LRB 2) and 1.80 and 1.99 $\times$ 10^{-3} (G+15), about 1.9 to 2.5 times the fixed-base first-storey drift (0.83 and 0.79 $\times$ 10^{-3}), and except for G+10 with LRB 1 it exceeds the maximum fixed-base drift of the building. This local peak, where the flexible isolation interface meets the frame, is reported separately in Table 2; drift values elsewhere in this study refer to the storeys above it. All drifts, including the first-storey peak, remain below the IS 1893 limit of 0.004.

Base shear decreases by 54.0% (LRB 1) and 46.4% (LRB 2) in the G+10 building but by only 44.2% and 44.3% in the G+15 building, because the taller frame already has a longer fixed-base period and a lower spectral acceleration, so lengthening the period to the same 3.0 s target removes a smaller share of the demand. A comparison of the two bearings supports this interpretation. In the velocity-controlled branch of the IS 1893 spectrum the spectral acceleration varies as 1/T, and for an isolated structure T varies as 1/√K, so base shear should scale approximately with √K. In the G+10 building LRB 2 is 1.48 times stiffer than LRB 1, and the scaling predicts a base shear ratio of 1.22 against an observed ratio of 1.17 (3,166.18/2,717.82 kN); in the G+15 building the two stiffnesses differ by 0.1% and the base shears by 0.2%. LRB 2 therefore performs worse in the G+10 building not because it is multilinear (in the RSA both bearings differ mainly in K_{eff}, Section 2.6) but because it is too stiff for the lighter building, a direct argument for height-specific proportioning.

Member forces follow the same pattern, but not uniformly. Column moments and shears, which are governed by lateral load, decrease by 49% and 44% (G+10, LRB 1) and by 42% and 32% (G+15, LRB 1). Beam B1 benefits much less: its moment falls by 21.1% (G+10) and 13.8% (G+15) and its shear by only 15.9% and 1.1%, because much of the beam demand comes from gravity load, which isolation does not change. For the same reason, the P-M-M ratios fall by only 17–26% with LRB 1 and by 2–5% with LRB 2.

These reductions are consistent with published results. The 54.0% base shear reduction of the G+10 building falls within the 50–70% range reported by Ziraoui et al.[1] for eight- and ten-storey RCC buildings on LRBs, while the 44.2% of the G+15 building is about six percentage points below it, consistent with its greater height. Domadzra et al.[2] reported a 65% drift

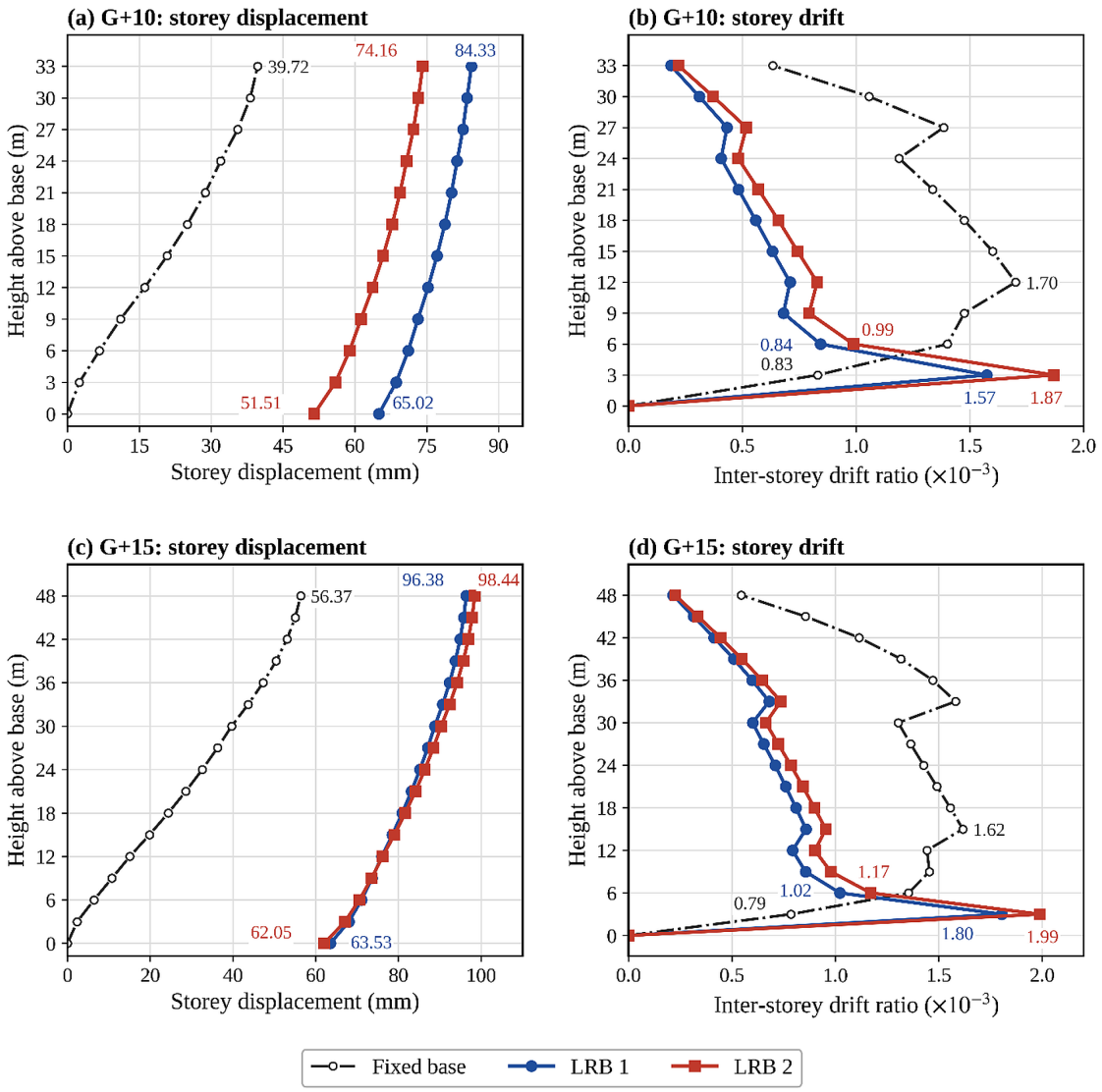

Fig 1. Healthy-condition storey displacement and storey drift profiles of the fixed-base, LRB 1 and LRB 2 models: (a, b) G+10 building; (c, d) G+15 building

reduction for a five-storey building from nonlinear time-history analysis; the smaller drift reduction obtained here (36.8–50.4% with LRB 1) is expected, because drift reduction diminishes as the superstructure becomes taller and more flexible. Haveri et al.[11] studied LRB isolation of a multi-storey RCC building under increased seismic demand, a case comparable with the healthy-bearing condition considered here.

3.2 Effect of aging on displacement, drift and base shear

As the bearings age, becoming stiffer and less damped, the displacement profiles move towards the fixed-base profile (Figure 2). In the G+10 building the roof displacement decreases from 84.33 to 76.74 mm with LRB 1 (−9.0%) and from 74.16 to 68.29 mm with LRB 2 (−7.9%). In the G+15 building it decreases from 96.38 to 90.15 mm (−6.5%) with LRB 1 and from 98.44 to 91.89 mm (−6.7%) with LRB 2, while the isolation-level displacement decreases more markedly, from 63.53 to 53.84 mm (−15.3%) and from 62.05 to 52.92 mm (−14.7%), respectively. These isolation-level ratios (0.847 and 0.853) are consistent with the base shear results: the bearing displacement equals the base shear divided by the bearing stiffness, and 1.100/1.30 = 0.846 for both bearings, which share the same base shear factor at 30% aging in the G+15 building (Table 3). The roof ratios (0.910 and 0.921

Table 2. Healthy (0% aging) response of fixed-base and isolated models; values in parentheses are reductions relative to the fixed-base model

Response quantity	G+10			G+15		
	Fixed base	LRB 1	LRB 2	Fixed base	LRB 1	LRB 2
Roof displacement (mm)	39.72	84.33	74.16	56.37	96.38	98.44
Isolation-level displacement (mm)	—	65.02	51.51	—	63.53	62.05
Max. inter-storey drift above first storey ($\times 10^{-3}$)	1.701	0.844 (50.4%)	0.988 (41.9%)	1.616	1.022 (36.8%)	1.171 (27.5%)
First-storey drift ($\times 10^{-3}$)	0.83	1.57	1.87	0.79	1.80	1.99
Base shear (kN)	5,911.86	2,717.82 (54.0%)	3,166.18 (46.4%)	7,061.98	3,941.02 (44.2%)	3,934.21 (44.3%)
Beam B1 moment (kN·m)	469.18	369.99 (21.1%)	444.08 (5.3%)	384.83	331.69 (13.8%)	337.04 (12.4%)
Column C1 moment (kN·m)	525.04	266.59 (49.2%)	320.84 (38.9%)	650.32	376.13 (42.2%)	389.54 (40.1%)
Column C2 moment (kN·m)	524.50	266.39 (49.2%)	320.82 (38.8%)	651.09	376.60 (42.2%)	390.06 (40.1%)
Beam B1 shear (kN)	237.50	199.83 (15.9%)	232.76 (2.0%)	232.11	229.66 (1.1%)	232.04 (0.0%)
Column C1 shear (kN)	199.83	112.78 (43.6%)	130.77 (34.6%)	239.21	162.43 (32.1%)	162.07 (32.2%)
Column C2 shear (kN)	199.56	112.47 (43.6%)	130.82 (34.4%)	240.04	162.45 (32.3%)	162.09 (32.5%)
P-M-M ratio, C1	0.508	0.378 (25.6%)	0.487 (4.1%)	0.688	0.549 (20.2%)	0.661 (3.9%)
P-M-M ratio, C2	0.599	0.472 (21.2%)	0.587 (2.0%)	0.788	0.654 (17.0%)	0.751 (4.7%)

for G+10, 0.935 and 0.933 for G+15) are higher because part of the roof displacement comes from the superstructure, whose deformation grows as the base shear rises.

Base shear and drift both rise almost linearly with aging (Figure 3, Table 3). At 30% aging the base shear of LRB 1 increases from 2,717.82 to 3,008.17 kN in the G+10 building (factor 1.107) and from 3,941.02 to 4,333.91 kN in the G+15 building (factor 1.100); the LRB 2 factors are 1.094 and 1.100. The maximum drift above the first storey increases by 10.7% and 9.2% (G+10, LRB 1 and LRB 2) and by 8.8% and 8.7% (G+15), and remains below 0.004 throughout. The mechanism is the reverse of isolation: a stiffer bearing shortens the isolated period and moves the structure up the descending branch of the spectrum, and the concurrent reduction in bearing damping acts in the same direction (Section 2.6). Period shift alone, through the p_K scaling, would give a factor of $p_{1.30} = 1.14$; the computed factors (1.09–1.11) are lower because the system period also depends on the flexibility of the superstructure, so a 30% change in bearing stiffness produces a smaller change in the system period. The base shear factor is well approximated by $1 + 0.36a$ for the G+10 building with LRB 1 ($1 + 0.31a$ with LRB 2) and by $1 + 0.33a$ for the G+15 building with either bearing. The step-to-step increments in Table 3 are not perfectly uniform (the G+10 LRB 1 drift factors rise in irregular steps of 0.011–0.024; the G+15 drift factor at 5% aging is 1.020 with LRB 1 but 1.010 with LRB 2, although the two bearings agree to within 0.001 at all other levels; and the first G+10 LRB 1 base shear step, 0.025, exceeds the later ones, 0.014–0.019). Because the reported drift is the maximum over all storeys above the first, small shifts in its storey distribution can produce such steps; they remain within ± 0.01 of a linear trend and do not affect the factors at 30% aging.

The factors for the two heights are similar, but the consequences are not. The G+10 building starts from a 54.0% base shear reduction and retains 49.1% at 30% aging (41.4% with LRB 2), whereas the G+15 building starts from 44.2% and retains 38.6% (38.7% with LRB 2). The residual margin against the fixed-base demand, which controls design, therefore explains the height dependence of aging better than the amplification factor does.

3.3 Effect of aging on member forces

Column moments and shears rise almost in proportion to the base shear (Figure 4 and 5). At 30% aging the column moment factors are 1.104 (LRB 1) and 1.090 (LRB 2) in the G+10 building and 1.097 for both bearings in the G+15 building, and the column shear factors are identical to three decimal places. The columns retain the main benefit of isolation: at 30% aging their

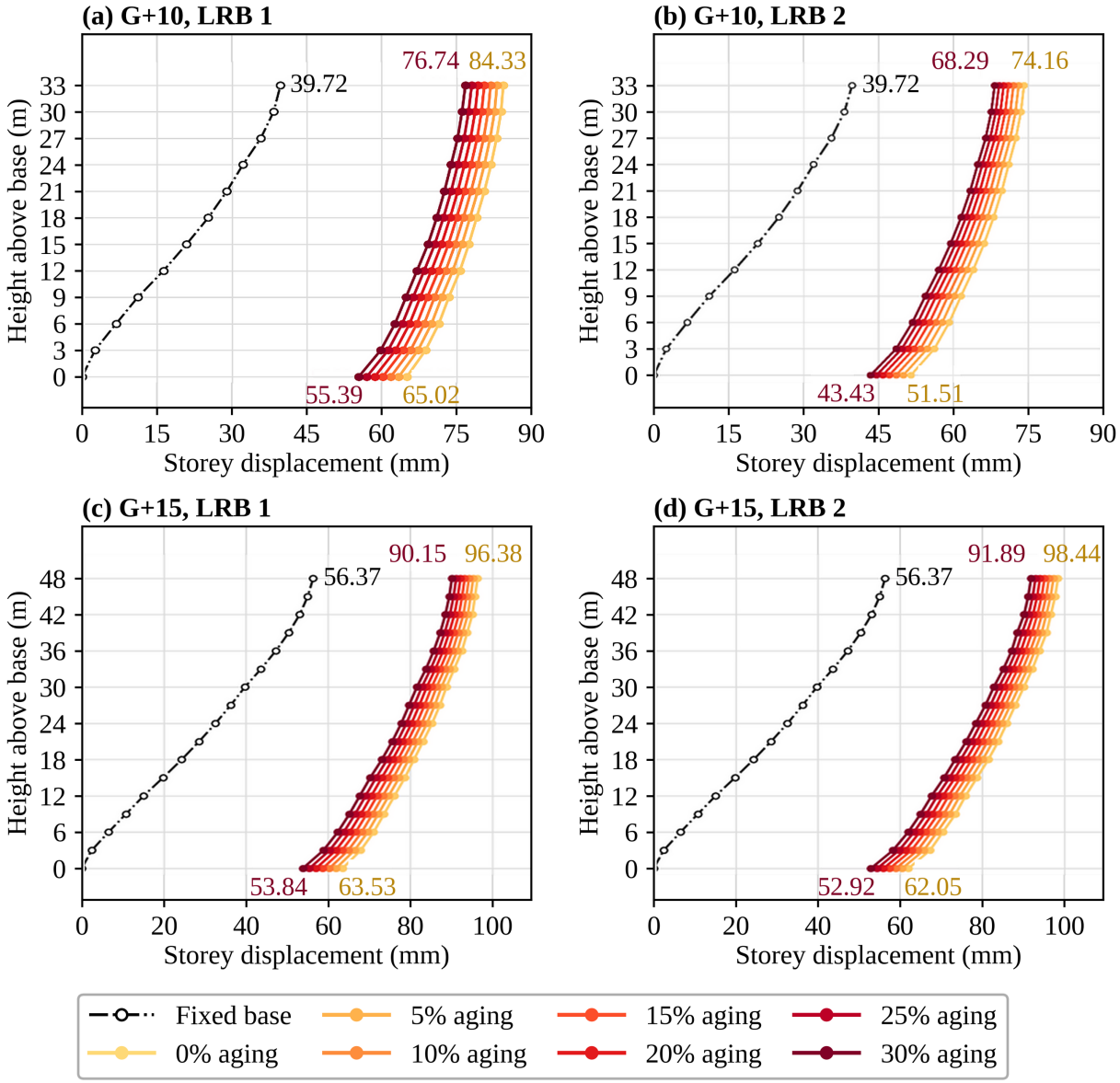

Fig 2. Storey displacement profiles at aging levels of 0–30% compared with the fixed-base profile: (a) G+10, LRB 1; (b) G+10, LRB 2; (c) G+15, LRB 1; (d) G+15, LRB 2

moments are still 43.9% (LRB 1) and 33.4% (LRB 2) below the fixed-base value in the G+10 building, and 36.5% and 34.3% below it in the G+15 building.

Beams are the critical members under aging because their initial margin is small (Table 3). In the G+10 building with LRB 1, the B1 moment increases from 369.99 to 405.33 kN·m at 25% aging and to 412.99 kN·m at 30% (factor 1.116), still 12.0% below the fixed-base value of 469.18 kN·m. With LRB 2 it remains marginally below the fixed-base value at 15% aging (461.7 kN·m), exceeds it at 20% (476.2 kN·m) and is 4.2% above it at 30%. The B1 shear retains a 7.8% reduction at 30% aging with LRB 1, but with LRB 2 it exceeds the fixed-base value from 10% aging onwards (6.4% above at 30%). With LRB 2 in the G+10 building, both B1 moment and shear change little between 10% and 15% aging and then rise more steeply (Figure 4a and 5a), a plateau that may result from a change in the governing load combination of the design envelope. In the G+15 building the B1 moment factor is 1.113 for both bearings, and the reduction decreases from 13.8% to 4.1% (LRB 1) and from 12.4% to 2.5%

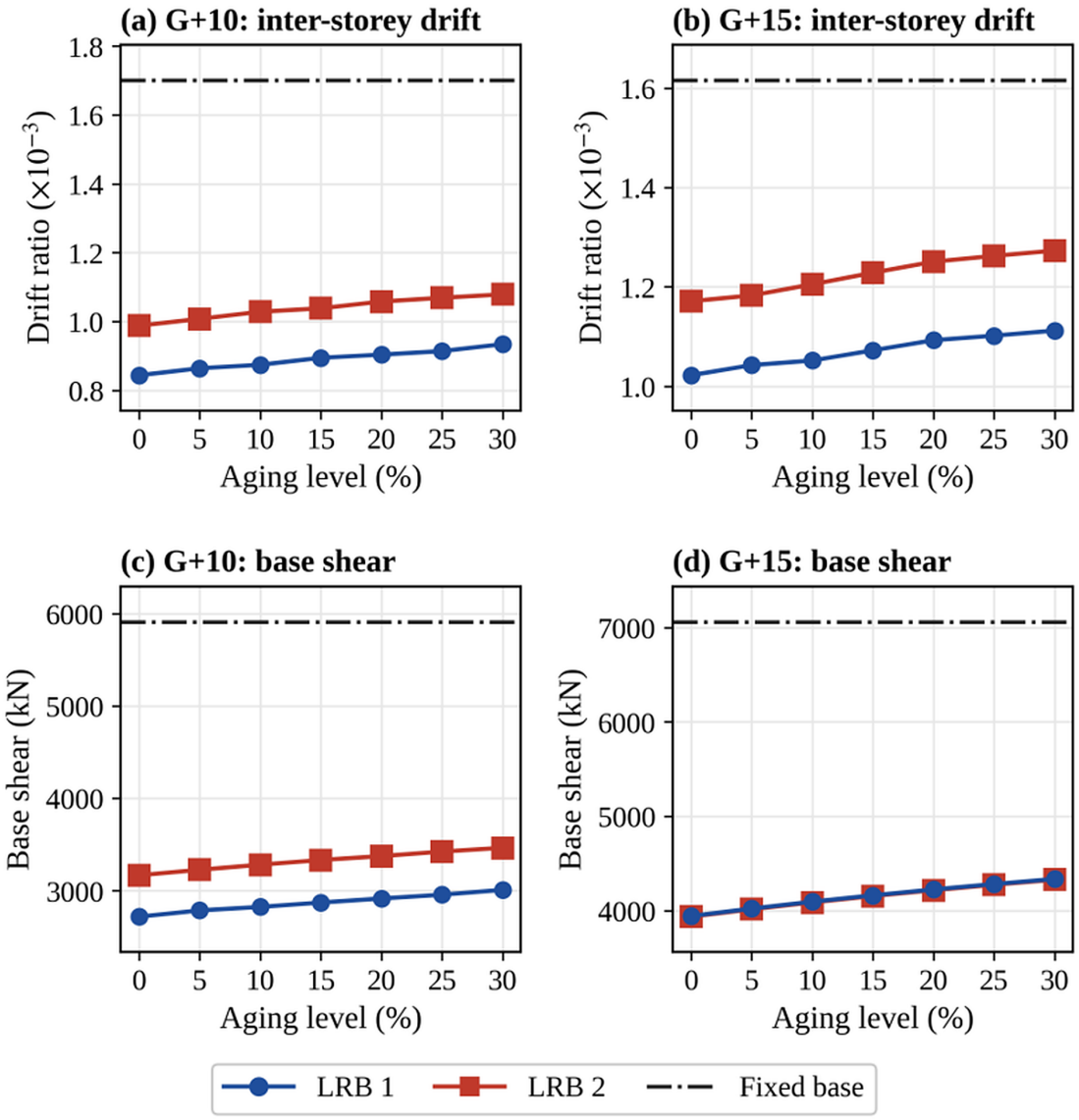

Fig 3. Effect of bearing aging on (a, b) maximum inter-storey drift above the first storey and (c, d) base shear of the G+10 and G+15 buildings

(LRB 2). The B1 shear, only 1.1% (LRB 1) and 0.0% (LRB 2) below the fixed-base value when healthy, exceeds it from 5% aging and is 6.6% (LRB 1) and 7.7% (LRB 2) above it at 30%. Beam forces in an isolated frame can exceed the fixed-base values, probably because isolation changes the height-wise distribution of lateral deformation as well as its magnitude, and B1 lies at the isolation level, directly above the bearings; once aging has consumed the small initial margin, this redistribution dominates. Beams designed for healthy-bearing forces may therefore be under-designed late in the service life, especially in taller buildings and with bearings not proportioned to the building.

3.4 Effect of aging on column P-M-M interaction ratio

The P-M-M ratios change by less than 2% over the full aging range (Figure 6). In the G+10 building they decrease from 0.378 to 0.371 (C1) and from 0.472 to 0.466 (C2) with LRB 1, and increase from 0.487 to 0.495 and from 0.587 to 0.596 with LRB 2. In the G+15 building they rise from 0.549 to 0.556 and from 0.654 to 0.662 with LRB 1, and from 0.661 to 0.671 and from 0.751 to 0.760 with LRB 2. The interaction check of these columns is thus controlled by gravity axial load rather than seismic moment:

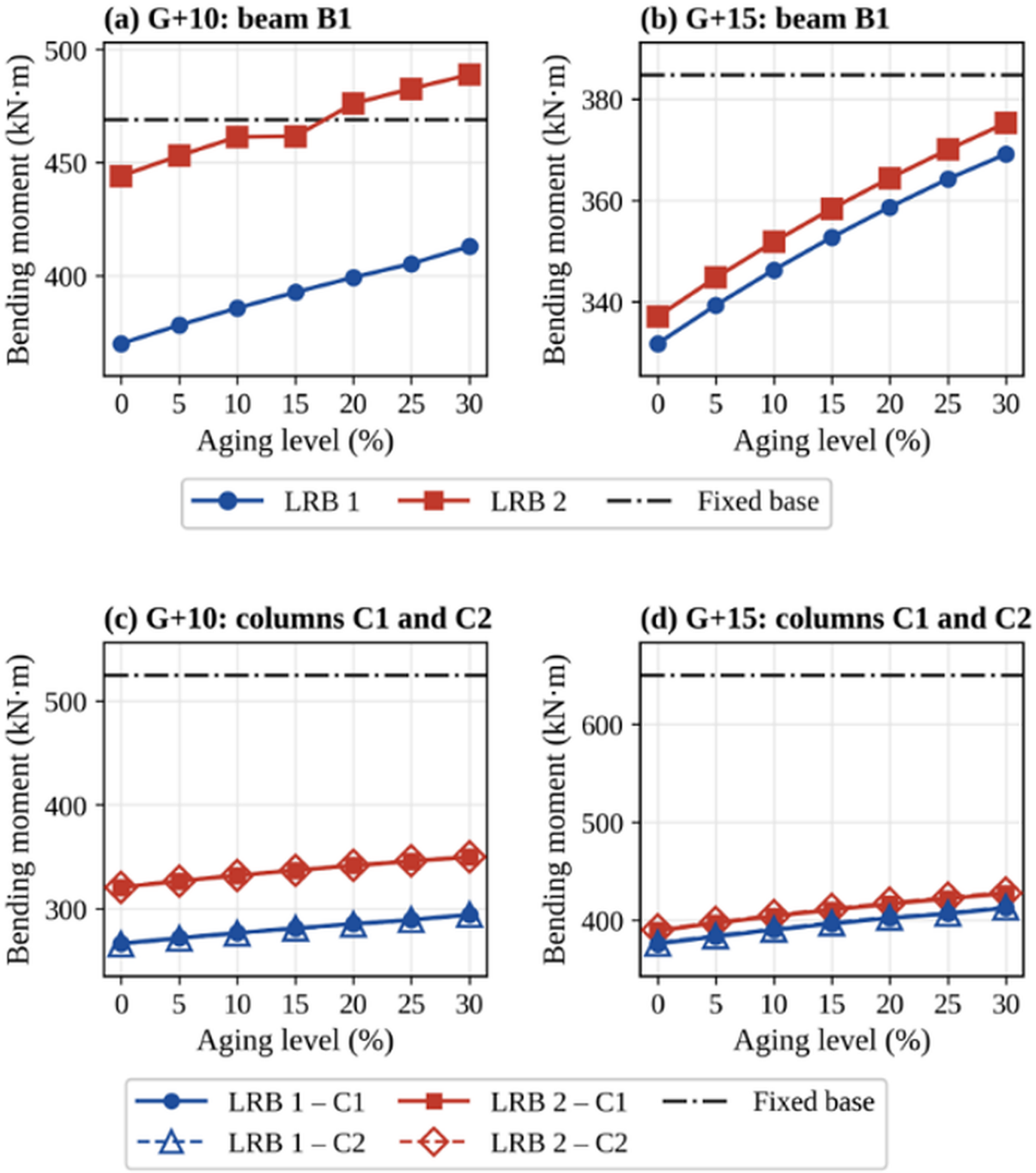

Fig 4. Effect of bearing aging on bending moment: (a, b) beam B1 and (c, d) columns C1 and C2 of the G+10 and G+15 buildings

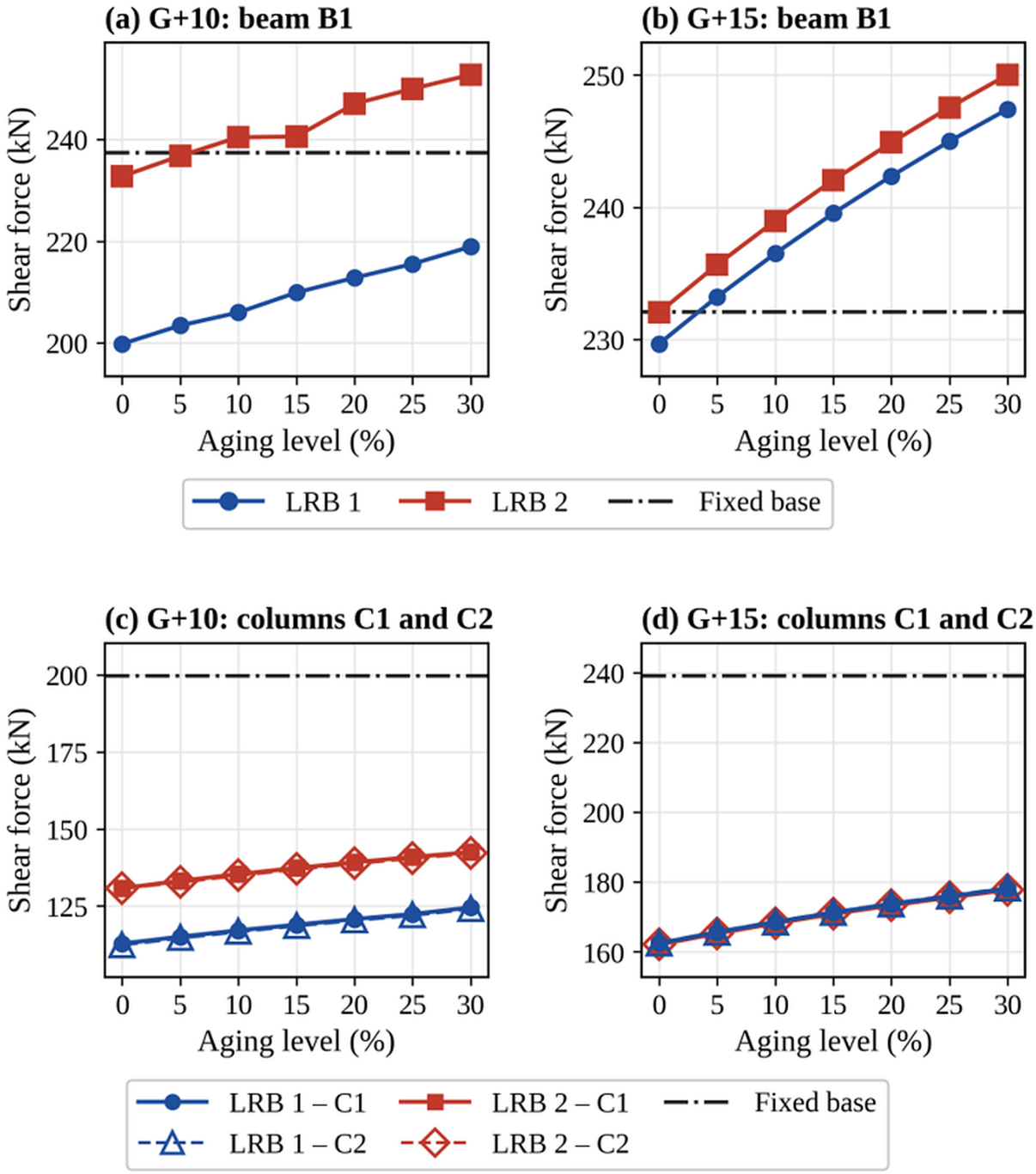

Fig 5. Effect of bearing aging on shear force: (a, b) beam B1 and (c, d) columns C1 and C2 of the G+10 and G+15 buildings

Table 3. Height- and configuration-specific aging modification factors (ratio of aged to healthy response, with the stiffness increase and damping reduction applied together); all factors are 1.000 at 0% aging

Aging level (λ_K, λ_ξ)	G+10		G+15	
	LRB 1	LRB 2	LRB 1	LRB 2
Base shear factor				
5% (1.05, 0.95)	1.025	1.019	1.020	1.020
10% (1.10, 0.90)	1.039	1.036	1.039	1.038
15% (1.15, 0.85)	1.056	1.052	1.056	1.056
20% (1.20, 0.80)	1.072	1.066	1.071	1.071
25% (1.25, 0.75)	1.088	1.081	1.086	1.086
30% (1.30, 0.70)	1.107	1.094	1.100	1.100
Inter-storey drift factor				
5% (1.05, 0.95)	1.024	1.020	1.020	1.010
10% (1.10, 0.90)	1.036	1.041	1.029	1.029
15% (1.15, 0.85)	1.060	1.051	1.049	1.049
20% (1.20, 0.80)	1.071	1.071	1.069	1.068
25% (1.25, 0.75)	1.083	1.082	1.078	1.078
30% (1.30, 0.70)	1.107	1.092	1.088	1.087
Beam B1 moment factor				
5% (1.05, 0.95)	1.022	1.020	1.023	1.023
10% (1.10, 0.90)	1.043	1.039	1.044	1.043
15% (1.15, 0.85)	1.061	1.040	1.063	1.063
20% (1.20, 0.80)	1.079	1.072	1.081	1.081
25% (1.25, 0.75)	1.096	1.087	1.098	1.097
30% (1.30, 0.70)	1.116	1.101	1.113	1.113
Beam B1 shear factor				
5% (1.05, 0.95)	1.019	1.016	1.016	1.015
10% (1.10, 0.90)	1.031	1.033	1.030	1.030
15% (1.15, 0.85)	1.051	1.034	1.043	1.043
20% (1.20, 0.80)	1.066	1.062	1.055	1.055
25% (1.25, 0.75)	1.079	1.074	1.067	1.066
30% (1.30, 0.70)	1.096	1.086	1.077	1.077
Column force factors at 30% aging (λ_K = 1.30, λ_ξ = 0.70)				
Column C1 moment and shear	1.104	1.090	1.097	1.097

a 10% rise in column moment changes the utilization by only 1–2%. The G+10 LRB 1 ratios are the only ones that fall slightly with aging, probably because the governing combination includes the seismic axial force: the larger overturning compression of the aged model moves the column along the lower branch of its interaction surface, where the moment capacity grows with axial load, so the utilization can fall although the moment rises. Every ratio stays far below 1.0, but the configuration effect is evident: at 30% aging LRB 1 keeps the columns 16–27% below the fixed-base utilization and LRB 2 only 0.5–3.6%, so that C2 of the G+10 building with LRB 2 (0.596) is nearly at the fixed-base value (0.599).

3.5 Height-specific modification factors and practical significance

For design, the findings can be summarized as multiplication factors. For λ_K = 1.30 combined with λ_ξ = 0.70, the healthy-bearing response of G+10-class buildings should be multiplied by about 1.11 for base shear and inter-storey drift above the first storey, 1.10 for column forces and beam shear and 1.12 for beam moments, and that of the G+15 class by about 1.10 for base shear and column forces, 1.09 for drift, 1.11 for beam moments and 1.08 for beam shear (LRB 1 values, which envelop those of LRB 2 at 30% aging; Table 3); intermediate aging levels can be interpolated linearly from Table 3. Roof displacement can be taken as 0.91–0.94 times the healthy value, but the isolation gap should be sized using the healthy value. Design based only

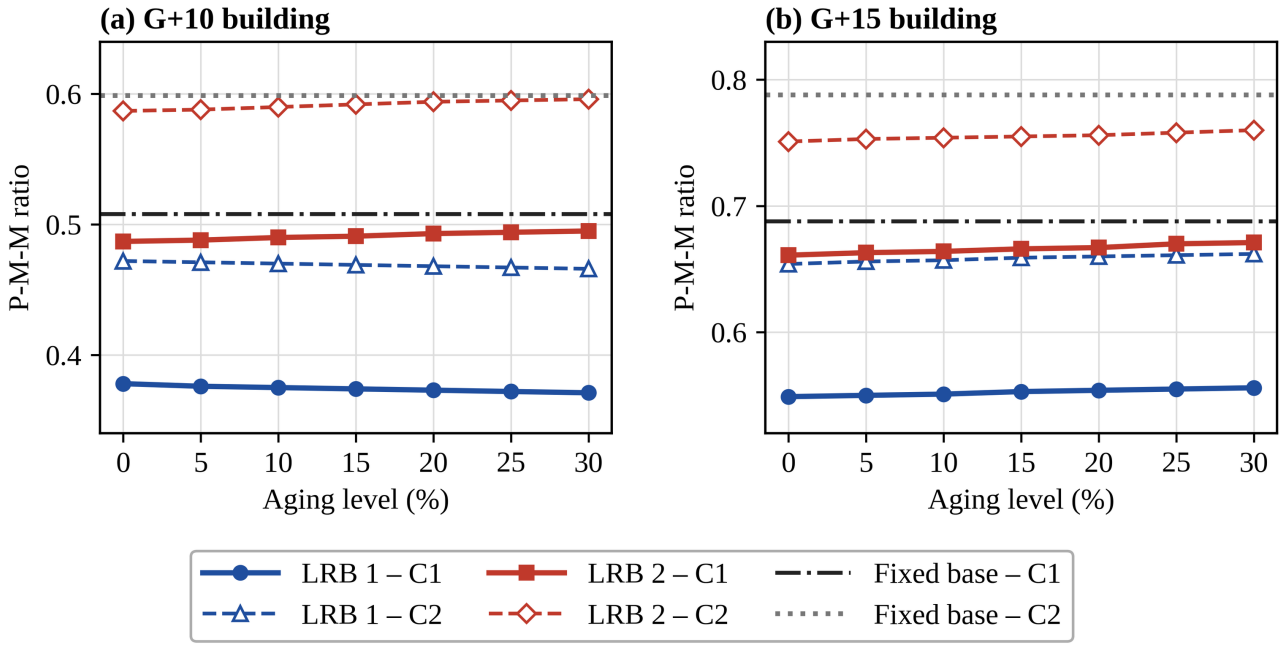

Fig 6. Effect of bearing aging on the P-M-M interaction ratio of columns C1 and C2: (a) G+10 building; (b) G+15 building

on as-manufactured properties therefore underestimates late-life superstructure forces by about 10%. Unlike earlier work on device aging[6],[7],[8], on a base-isolated reactor building[12] or on one building with a different bearing type[9], these factors relate device aging directly to the response of LRB-isolated RCC frame buildings of different heights. Two points follow for practice: a height-specific bearing (LRB 1) is markedly more tolerant of aging than a standard bearing that is too stiff for the building, because it starts from a larger margin; and inspection and replacement planning should be based on the residual margin, which is lowest for the beams of the taller building, rather than on the amplification factor.

4 Conclusion

Equivalent-linear Response Spectrum Analysis was used to assess the seismic response of G+10 and G+15 RCC buildings isolated with two LRB configurations at seven bearing aging levels (0–30%), each combining an increase in isolator effective stiffness with an equal percentage reduction in damping. The main conclusions are as follows.

1. Compared with the fixed-base model, healthy LRB 1 reduced base shear by 54.0% (G+10) and 44.2% (G+15) and the maximum inter-storey drift above the first storey by 50.4% and 36.8%, although the first-storey drift directly above the isolation plane was 1.9–2.5 times the fixed-base value. The smaller benefit in the taller building results from its longer fixed-base period.
2. Aging, represented by λ_K = 1.00–1.30 and λ_ξ = 1.00–0.70, produced approximately linear increases in base shear, drift and column forces. At 30% aging the LRB 1 factors for the G+10 and G+15 buildings were 1.107 and 1.100 for base shear, 1.107 and 1.088 for drift above the first storey and roughly 1.10 for column forces, while roof displacement dropped by 9.0% and 6.5%, respectively. Because superstructure flexibility limits the change in system period, these combined stiffness–damping factors fall below the simple period-shift estimate of $\mathrm{P}1.30 = 1.14$.
3. At 30% aging, isolation remained effective: base shear was still 49.1% (G+10) and 38.6% (G+15) below the fixed-base value, column moments with LRB 1 were 36–44% below it, drift stayed below 0.004 and all P-M-M ratios remained below 1.0.
4. Beams are the members most sensitive to aging, and the height dependence of aging lies mainly in the residual margin: the taller building starts with a smaller benefit, which a similar amplification consumes sooner. Beam moment factors at 30% aging were 1.116 (G+10) and 1.113 (G+15), the highest of any response quantity. In the G+15 building beam shear exceeded the fixed-base value from 5% aging onwards and beam moments retained only 2.5–4.1% reduction at

30% aging; with the stiffer LRB 2, the G+10 beam shear and moment exceeded their fixed-base values from 10% and 20% aging, respectively. Beam design should account for aged bearing properties.

5. Aging tolerance depends on the bearing configuration. In the G+10 building, where LRB 2 is 48% stiffer, the height-specific LRB 1 performed better than the standard LRB 2, but in the G+15 building, where their stiffnesses match, the two performed nearly identically.

The study converts bearing-level aging into height- and configuration-specific aging modification factors for LRB-isolated RCC buildings. Design based solely on as-manufactured bearing properties is about 10% non-conservative, beams at the isolation level are the members most at risk, and bearings should be proportioned to the building height and mass if isolation is to remain effective throughout the service life. The factors combine the specified stiffness increase and damping reduction of the bearings; they apply only to the buildings, site conditions and aging levels studied and should not be generalized without further validation.

This study has several limitations. The equivalent-linear RSA, with effective stiffness and damping evaluated once for the healthy bearing and then scaled for aging, does not capture the displacement dependence of these properties, lead-core heating or superstructure nonlinearity, and the effect of aging on the first-storey drift peak was not evaluated. The separate contributions of the stiffness increase and the damping reduction were not isolated. Aging is imposed as a uniform, parametric change in stiffness and damping, not related to non-uniform aging through the bearing or to calendar time. There was no experimental or field validation, and only two regular buildings, one seismic zone and one soil type were considered. Future work should verify the factors by nonlinear time-history analysis, including near-fault motions under which LRB damage has been reported[13]; check the assumed property changes against accelerated-aging tests or bearings recovered from service; extend the range to aging above 30%, other zones and soils, irregular and taller buildings and soil–structure interaction; and evaluate the life-cycle cost of bearing replacement.

5 Acknowledgements

NIL

Author details: Adersha Babu is a M.Tech. Student; Dr. Chethan Gowda R K is an Associate Professor.

References

1) Ziraoui A, Kissi B, Aaya H, Azdine I. Seismic behavior of base-isolated building structures with lead rubber bearings (LRBs). *Procedia Structural Integrity*. 2024;61:171–179. https://doi.org/10.1016/j.prostr.2024.06.023.
2) Domadzra Y, Bhandari M, Hasan M. Influence of characteristics of lead rubber bearing isolator on the seismic response of a base-isolated building. *Journal of Structural Design and Construction Practice*. 2025;30(3):04025044. https://doi.org/10.1061/JSDCCC.SCENG-1737.
3) Kayı DB, Bayhan B, Özdemir G. Effect of superstructure characteristics on seismic response of an RC building retrofitted with lead rubber bearings. *Bulletin of Earthquake Engineering*. 2026;24(8):6413–6441. https://doi.org/10.1007/s10518-026-02466-0.
4) Yanik A, Okuroğlu D. Comparative seismic performance of LRB and HDRB systems in reinforced concrete buildings. *Asian Journal of Civil Engineering*. 2026;27:4275–4283. https://doi.org/10.1007/s42107-026-01722-7.
5) Madhukumar M, Santhi MH, Vasugi V. Performance analysis of lead rubber bearing isolation system for low, medium and high-rise RC buildings. *Research on Engineering Structures and Materials*. 2023;9(1):263–276. https://doi.org/10.17515/resm2022.437ie0526.
6) Sánchez MAG, Giraldo-Vásquez DH, Sánchez RM. The effect of thermal ageing on the mechanical properties of natural rubber-based compounds used for rubber bearings. *Construction and Building Materials*. 2021;287:123012. https://doi.org/10.1016/j.conbuildmat.2021.123012.
7) Li Y, Ma Y, Zhao G, Liu R. Study on the basic performance deterioration law and the application of lead rubber bearings under the alternation of aging and seawater erosion. *Ocean Engineering*. 2023;281:115167. https://doi.org/10.1016/j.oceaneng.2023.115167.
8) Velasco-Cuervo IC, Rueda-Almonacid DA, Caicedo B, Buitrago J. Impact of aging and low temperatures on the mechanical properties of low-cost seismic isolator prototypes. *Buildings*. 2025;15(13):2238. https://doi.org/10.3390/buildings15132238.
9) Calabrese A, Losanno D, Barjani A, Spizzuoco M, Strano S. Effects of the long-term aging of glass-fiber reinforced bearings (FRBs) on the seismic response of a base-isolated residential building. *Engineering Structures*. 2020;221:110735. https://doi.org/10.1016/j.engstruct.2020.110735.
10) Xue B, Lu W, Ren X, Wen W. A hysteretic model of lead-rubber bearings considering coupled thermal and mechanical behavior. *Journal of Building Engineering*. 2025;103:112118. https://doi.org/10.1016/j.jobe.2025.112118.
11) Haveri M, Tuppad N, Gowda RKC. Numerical investigation on the seismic performance of a multistorey RC building under increased seismic demand using lead rubber bearing isolation. *Indian Journal of Science and Technology*. 2026;19(25):1729–1739. https://doi.org/10.17485/IJST/v19i25.944.
12) Rahman MM, Nahar TT, Kim D, Park DW. Seismic performance evaluation of base-isolated nuclear power plant reactor building considering aging effect of isolation device. *Journal of Nuclear Science and Technology*. 2022;59(12):1465–1477. https://doi.org/10.1080/00223131.2022.2063959.
13) Ren Y, Wang R, He W, Liu W. Numerical simulation analysis of lead rubber bearings (LRBs) damage and superstructure response under near-fault earthquakes. *Buildings*. 2025;15(5):839. https://doi.org/10.3390/buildings15050839.